Biological Adsorption and Desorption of Anionic Congo Red Dye by Nano Composite Polymer Sheets

CrossMark

Hagar M Magdy[1], Hekmat R Madian[1], Ahmed E Abdelhamid[2], Notiala Naseer[1], Mahmoud M Hegazi[3], Ahamed Labena[1*]

1- Egyptian Petroleum Research Institute (EPRI), Nasr City 11727, Cairo, Egypt
2- Polymers & Pigments Dept, National Research Centre (NRC), Dokki, Cairo, 12622, Egypt
3- Agricultural Engineering Dept, Fac of Agric, Ain Shams Univ, P.O. Box 68, Hadayek Shoubra 11241, Cairo, Egypt

*Corresponding author: a.labena@epri.sci.eg

Abstract: Congo red (CR) is an anionic dye that is released from various industries and demonstrates a negative effect on the environment and human health. Dye`s elimination from the environment is an important challenge; therefore, the aim of this study was the application of unhydrolyzed sugarcane bagasse wastes, after acid hydrolysis, drying, grinding and including cellulose acetate to form different composite sheets. The composite sheets were applied in the 3Rs (Removal of Congo red using the composite sheet, Recover of the Congo red after removal using ethanol, and Reuse of the composite sheet many times) processes. The Congo red removal efficiency by the composite sheets was optimized using two statistical methods, One Factor at A Time (OFAT) and General Factorial Design. Afterward, isotherms models and kinetics studies were investigated; moreover, the reusability was also examined. The results exhibited that, the Congo red removal efficiency of 76.27 % was achieved for 500 ppm of the dye using the composite sheet with a concentration of 7 g/L; at a pH value of 7.0 and a contact time of 240 min. Interestingly, the composite sheets have been applied for 3Rs (Removal, Recovery, Reuse) cycles 5 times.

1 Introduction

Congo red (CR) is an anionic dye that is industrially applied as a coloring agent. Moreover, this dye may be generated from the waste of various industries such as rubber, plastics, paper, tanning and pharmaceuticals industries (Rafatullah et al 2010). This dye when discharged into a water stream without treatment leads to a plethora of environmental and human-being problems (Javadian et al 2013). The CR dye-containing effluent is responsible for many diseases in human beings like skin irritation, allergy and dermatitis. Therefore, different physico-chemical techniques were investigated to help such industries in the elimination of the CR from their effluents before discharging. However, these techniques had a lot of drawbacks e.g. their high cost and the generation of hazardous wastes after the treatment process (Moghazy 2019, Husien et al 2019a, Husien et al 2019b). The adsorption method, generally and specifically using agriculture biomasses such as sugarcane bagasse wastes is the most preferable method that can overcome these problems (Kant 2011, El-Jamal and Ncibi 2012).

Worldwide, Egypt is rated as the sixteenth in sugarcane bagasse usage and thus sugarcane bagasse wastes are nominated as the highest biomass in Egypt (Kamran et al 2022) and have been used for a long time in the production of bioethanol (Abo-State et al 2013, Ajala et al 2021). The production of bioethanol from these wastes needs a pre-treatment process. This pre-treatment by acid and/or base is crucial to degrade the lignin content and free the cellulose and hemicellulose contents (Morán-Aguilar et al 2022). Afterward, the residual unhydrolyzed wastes afford a highly charged material that can be used as an excellent sorbent. However, the application of these wastes, in their produced form with a low surface area, predicts a low removal efficiency and prevents the replicability option (Moghazy et al 2019). In addition, the next challenges that face scientists nowadays are how to collect the materials after treatment, how to recover the adsorbed dye from the sorbent material and how many times that can be used. These challenges should lead to tailoring an economic product with many useful features as previously reported (Prabhu et al 2017, Munagapati et al 2020).

Therefore, in this study, sugarcane bagasse wastes were collected from the local market and treated with acids as a pre-step-in bioethanol production. The acid treatment materials were distinguished as (1) 20g bagasse with 2% H_2SO_4, (2) 20g bagasse with 4% H_2SO_4, (3) 10g bagasse with 4% H_2SO_4, and (4) 10g bagasse with 4% H_2SO_4. The unhydrolyzed wastes, after acid treatment, were dehydrated and ground. The ground material`s size was characterized by Dynamic Light Scattering (DLS) and identified by Fourier transform infrared (FT-IR) to detect its main functional groups. The ground unhydrolyzed sugarcane bagasse wastes were incorporated into a cellulose acetate forming various composite sheets. The composite sheets (1, 2, 3, 4) in addition to a blank composite sheet (cellulose acetate without any unhydrolyzed sugarcane bagasse wastes) and a control composite sheet (cellulose acetate untreated sugarcane bagasse wastes) were applied in the removal of an ionic dye, Congo red from synthetic contaminated water. The removal process was established *via* a batch experiment and optimized *via* two statistical models; One Factor at A Time (OFAT) and subsequently general factorial design. Moreover, isotherm models and kinetics studies were performed to demonstrate the mechanism of the adsorption reaction. After obtaining the optimum conditions that achieve the highest CR removal efficiency, the composite sheets were applied in a sequence process named

(3Rs); removal of CR, recovery of CR *via* treatment with ethanol and reuse again many times to check their applicability and reusability options.

2 Materials and Methods

2.1 Sorbent preparation, characterization and composite sheet formation

The sugarcane bagasse wastes were collected and dried. The materials were afterward stored in plastic bags at room temperature until analyses and treatment. Two concentrations of the sugarcane bagasse waste (10 and 20 g) were mixed separately with 100 ml of different concentrations of H_2SO_4 (2% and 4% v/v). Each treatment was autoclaved for 20 min, filtered and dried. The residual unhydrolyzed sugarcane bagasse wastes were distinguished as 1,2,3 and 4. The unhydrolyzed wastes were ground to the smallest size using a ball mailing (" Planetary Ball Mill PM 400, Malvern UK"). Subsequently, the ground waste's size was estimated by Dynamic Light Scattering (DLS) (" Zeta size Nano Series HT, Nano-25, Malvern UK"). The ground material`s functional groups were estimated using FT-IR spectroscopy ("Nicolet IS-10 spectroscopy"). Afterward, 1.8 gm of cellulose acetate was dissolved in 10 m of Dimethylformamide (DMF) (Abdelhamid and Khalil 2019). The unhydrolyzed wastes were added separately to the solution, stirred, and left to form a uniform mix. Consequently, the solution was cast onto a clean glass plate forming various composite sheets. The composite sheets (1, 2, 3, 4) in addition to a blank composite sheet (cellulose acetate without any unhydrolyzed sugarcane bagasse wastes) and a control composite sheet (cellulose acetate untreated sugarcane bagasse wastes) were applied in the removal of an ionic dye, Congo red (CR) from synthetic contaminated water.

2.2 Adsorption batch preparation

The CR stock solution was prepared at a concentration of 1000 ppm. After that, serial dilutions of 100, 200, 300, 400 and 500 ppm, were achieved upon use.

2.3 Screening experiment

A 1 g/l from each composite sheet was placed in the CR solution and shaken for 3h at 100 rpm as a screening experiment. At the end of the experiment, the CR initial and final concentrations were checked by spectroscopy (Cary 100 UV/Vis) at a wavelength of 497 nm as follows:

$$Removal\ effeciency\ (\%) = \frac{c_o - c_e}{c_o} \times 100$$

Where C_o is the initial CR concentration, C_e is the final CR concentration.

2.4 Optimization steps

Two optimization steps; "On Factor at a Time (OFAT)" (to determine the high and low levels) and "general full factorial design" were used in the CR removal using the composite sheets.

2.4.1 OFAT experiments

Different contact times were investigated; 30, 60, 90-, 120-, 180- and 240-min. Different pH values were evaluated; 3, 5, 7 and 9. Different dosages of the composite sheets (1, 2, 3 and 4) with amounts of 2, 5 and 7 g/l were also investigated. Moreover, different Congo red concentrations 100, 200, 300 and 500 ppm were also determined.

2.4.2 General Full factorial design experiments

23^31 general full factorial design experiments were used for the selected composite sheets to obtain the best factors that give high removal efficiency; **Tables S1 and S2** report the levels of the factors. The design matrix provides the obtained CR removal efficiency with fits and residual values. From the design experiments, the interaction between factors was estimated to obtain the interactive and effective variables that display the CR highest removal efficiency using the composite sheets. Different factors were examined; dye concentration, pH values, composite sheet dose, and contact time. The main and interaction effects, Pseudo-chart and Response optimizer were Figured out. The data were measured by Minitab 18 software with one replicate.

2.5 Langmuir and Freundlich isotherms

For the aim of the CR adsorption mechanism determination by the selected composite sheets as adsorbent materials, the linear Langmuir and Freundlich isotherms were examined as previously reported (Freundlich 1907, Langmuir 1918).

2.6 Kinetics studies

These studies were performed to investigate the rate of CR adsorption by the selected composite sheets, which are controlled by an equilibrium time. The kinetics models include the pseudo-first-order (1st) and the pseudo-second-order (2nd) according to Weber and Morris (1963) and Ho et al (2000).

2.7 Reusability experiment

After the implementation of the optimization process, the optimum factors were reinvestigated to confirm the result of the response optimizer and perform the reusing experiment. Ethanol concentrations of 100% were used to check the reusability of the selected composite sheets. The results were plotted and explained as 3Rs (Removal, Recovery and Reuse) of the composite sheets for many runs.

3 Results and discussion

3.1 Characterizations of the ground wastes

The size of the ground wastes was determined using DLS. The results displayed that the average size was 295.8, 286.8, 455, 116 and 291.4 nm for the control, 1, 2, 3 and 4, respectively as presented in **Fig S1**. The FT-IR spectra of the ground unhydrolyzed wastes were displayed in **Figs S2a, b, c, d and e**, respectively. The results showed that all wastes demonstrated several characteristic peaks for a cellulosic structure such as peaks around 3385, 1224, 2914 and 2865 cm^{-1}, which related to OH stretching, OH bending out of a plane, CH_2 and CH stretching vibrations, respectively. The peak around 1720 cm-1 represented a carbonyl band (C=O) of carboxylic acid or ester. The peaks around 1375, 1460 and 1057 cm^{-1} were related to CH_3, CH_2 bending and C-O stretching, respectively.

3.2 Application of the composite sheets in the removal of Congo red (CR) from contaminated wastewater

3.2.1 Screening experiment

Fig 1 displayed the initial screening experiment for the Congo red removal using the blank sheet (polymer without any unhydrolyzed bagasse wastes), the control sheet (polymer with the bagasse substrate without any acid treatment) and the four composite sheets (1, 2, 3 and 4) performed from unhydrolyzed sugarcane bagasse wastes. The results demonstrated that the composite sheets 1, 3 and 4 displayed removal efficiencies of 35.6, 29.3 and 26.1 for the CR compared to the composite sheet 2, the blank and control sheets. Therefore, these sheets were selected for further optimization process.
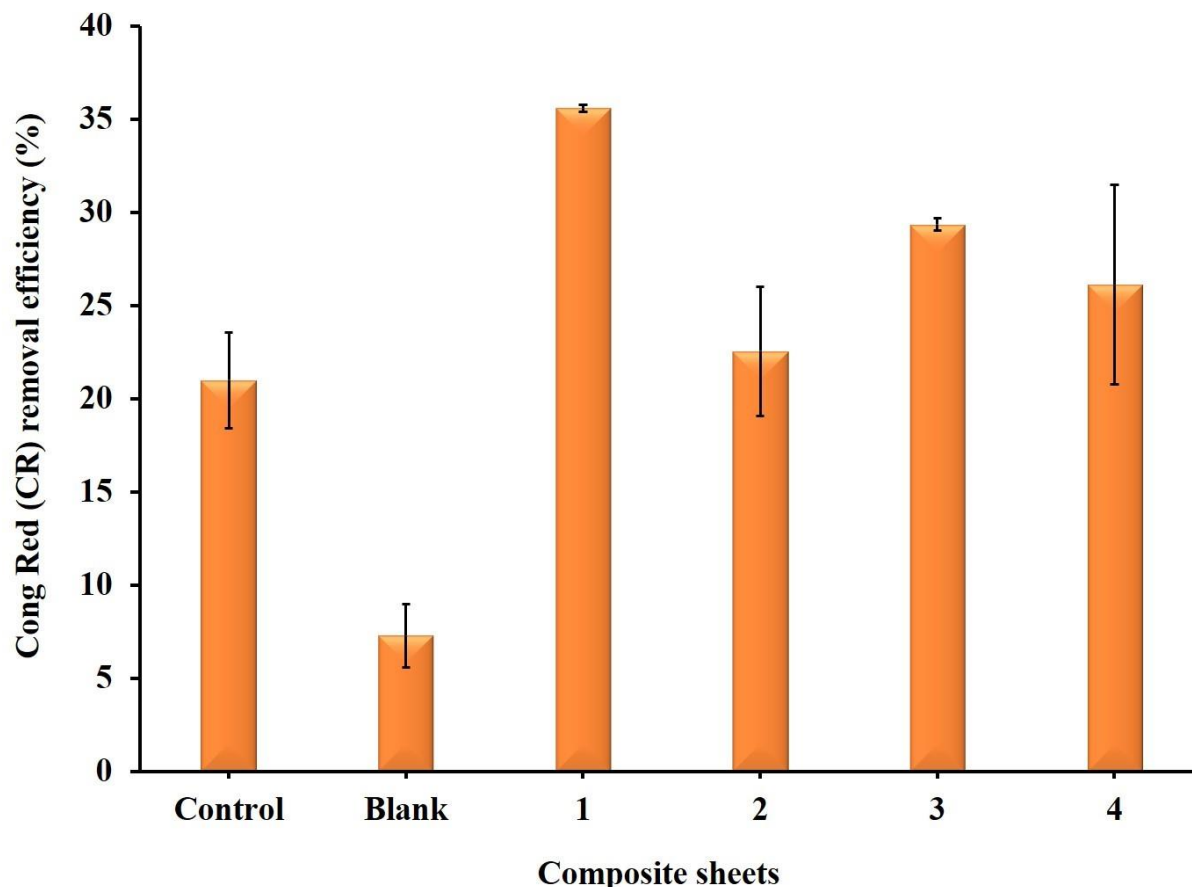
Fig 1. Screening of the composite sheets to select the highest Congo Red (CR) removal efficiency

3.2 Optimization process

3.2.1 OFAT experiments

Optimum levels, low and high, for the selected factors, were expressed in **Table S1, Fig 2** shows the correlation between different contact time intervals and the Congo red (CR) removal efficiency by the selected composite sheets (1, 3 and 4). The results demonstrated that the highest CR removal efficiencies of 25.9 and 44.6 %, respectively were achieved for the composite sheet 1 and 4 after 240 min. However, it was after 180 min for the composite sheet 3 with a removal efficiency of 34.1% (Nandi et al 2009).

The correlation between the pH values and the CR removal efficiencies is displayed in **Fig 3**. The highest removal efficiencies were achieved at a pH value of 5.0 for composite sheet 1 and 6.5 for composite sheets 3 and 4. This result was probably correlated to the increase in negativity charges of the solution which leads to a repulsion process and hence increases the removal efficiency.

Furthermore, it was reported that an increase in sorbent dose expedites an increase in the available active sites that further reflect a higher removal percent of the pollutant (Alver and Metin 2012). However, this reasonable behavior can be displayed up to a specific sorbent concentration; afterward, there is a stability attitude or a decrease in the adsorption process as previously reported (Cho et al 2003). The correlation between the composite sheet`s dose and the CR removal efficiencies is displayed in **Fig 4.** The highest removal efficiencies were obtained at the composite sheet`s concentration of 5 g/L.

Moreover, the correlation between the initial dye`s concentration and the CR removal efficiencies is displayed in **Fig 5**. The results showed that 100 ppm of the CR gave the highest removal efficiencies of all composite sheets. By increasing the dye concentration, the removal efficiencies were decreased as previously reported (Alver and Metin 2012). Finally, composite sheet 4 displayed the highest CR removal efficiency (Beltrán-Heredia and Sánchez-Martín 2008).

Table 1. ANOVA table of the selected composite sheets; 1, 3, 4 (treats) optimizations for the CR removal efficiency

| Source	DF	Adj SS	Adj MS	F-Value	P-Value
Model	10	45.532	4.55	12.36	0.000
Linear	5	35.159	7.038	19.09	0.000
CR Conc. (ppm)	1	25.106	25.10	68.17	0.000
Composite sheets (Treat)	2	3.993	1.99	5.42	0.019
Dose (g/l)	1	3.503	3.50	9.51	0.009
Time	1	2.556	2.55	6.94	0.021
2-Way Interactions	5	10.373	2.07	5.63	0.006
CR Conc. (ppm)*Treat	2	7.168	3.58	9.73	0.003
Composite sheets (Treat)*Time	2	1.678	0.83	2.28	0.142
Dose (g/l)*Time	1	1.526	1.52	4.14	0.063
Error	13	4.787	0.36		
Total	23	50.319			
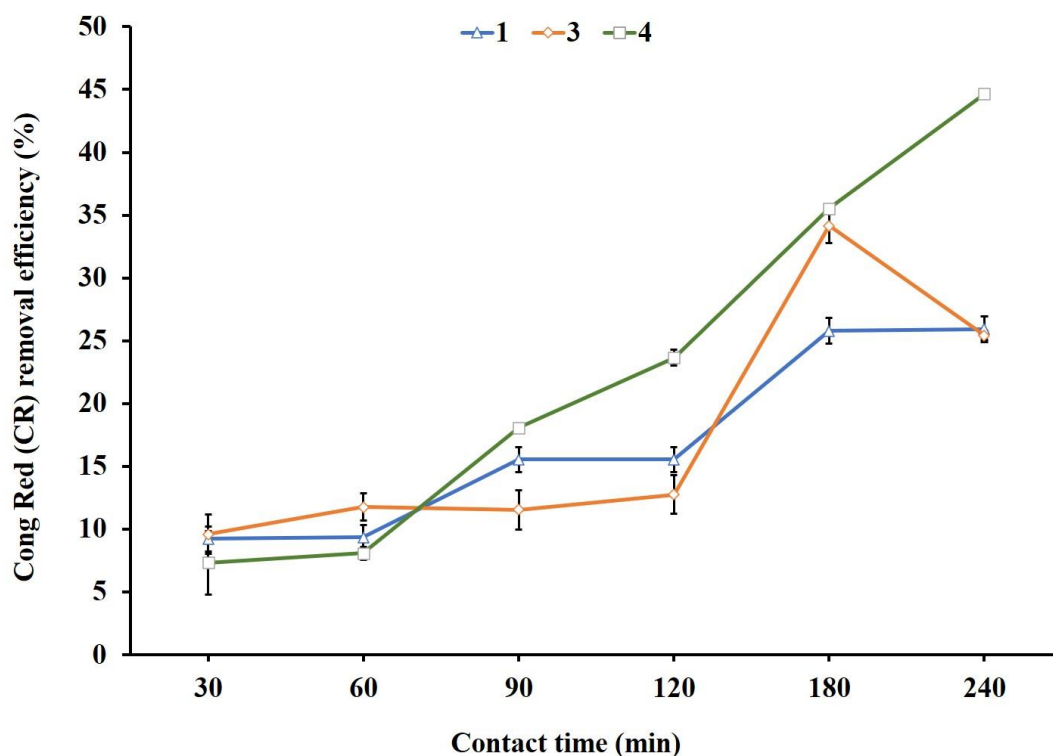
Fig 2. The correlation between contact time intervals and the Congo Red (CR) removal efficiencies using the selected composite sheets (1, 3 and 4)
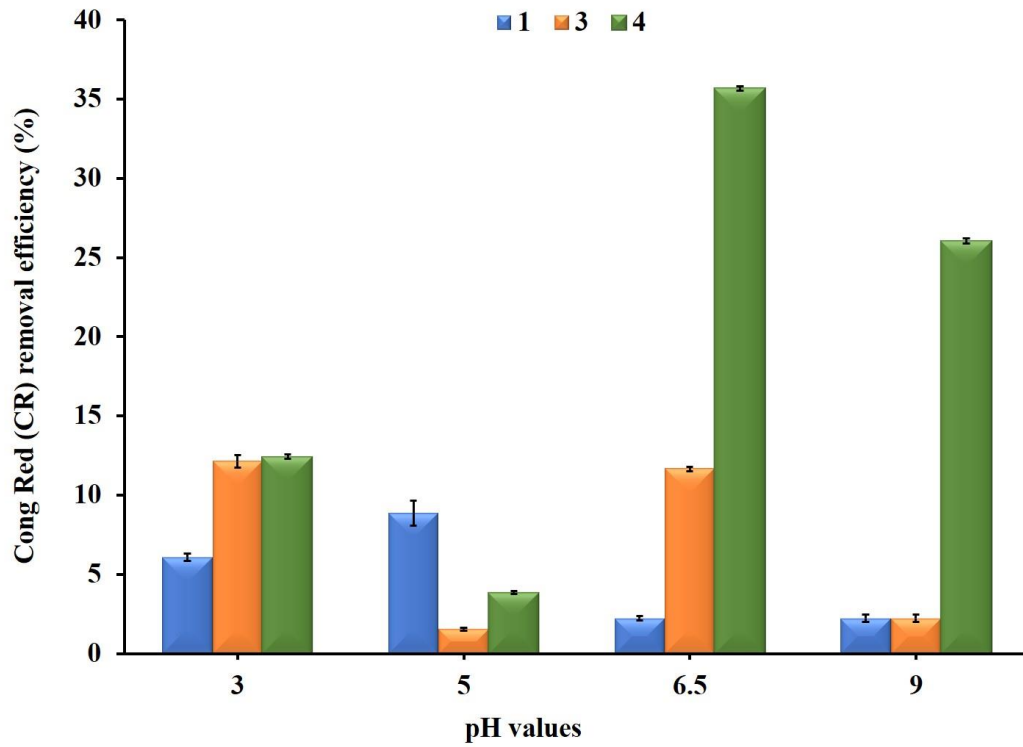
Fig 3. The correlation between pH values and the Congo Red (CR) removal efficiencies using the select composite sheets (1, 3 and 4)
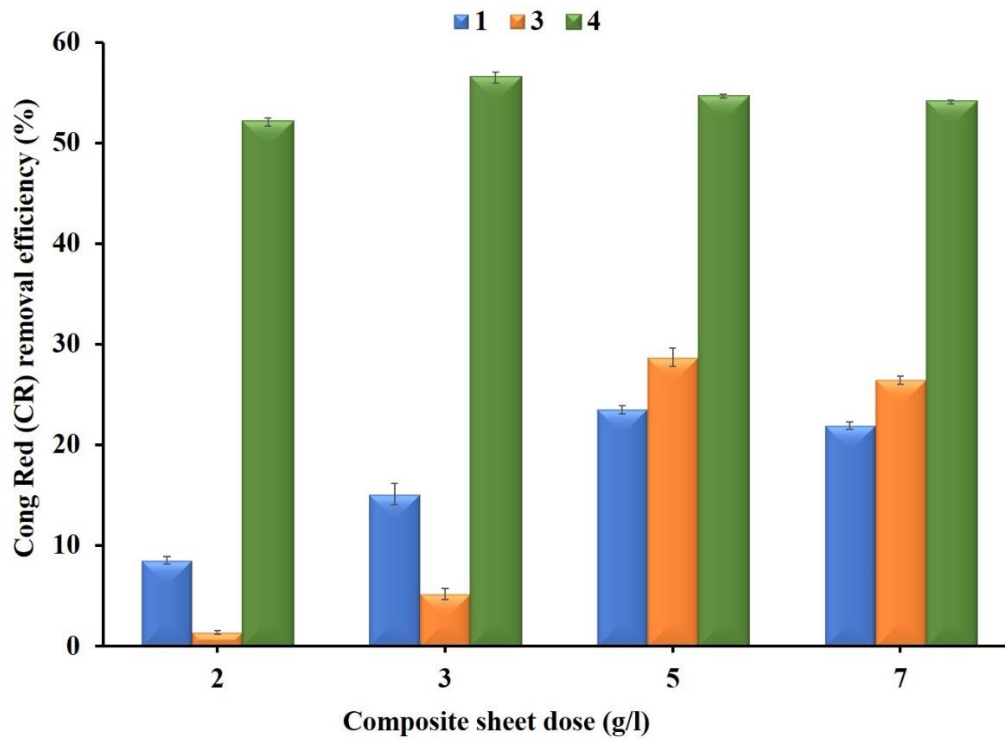

Fig 4. The correlation between the composite sheet`s dose and the Congo Red (CR) removal efficiencies using the selected composite sheets (1, 3 and 4)
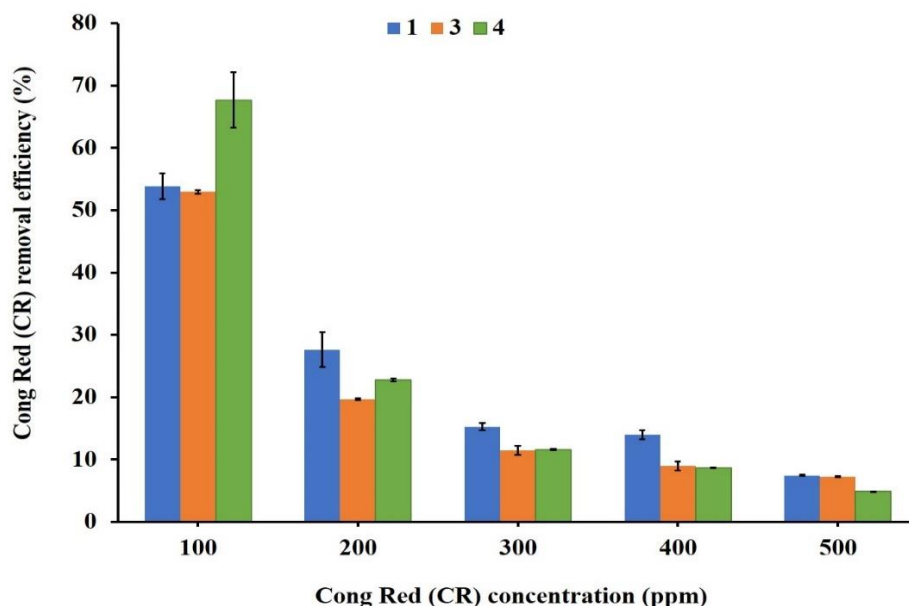
Fig 5. The correlation between dye`s concentration and the Congo red (CR) removal efficiencies using the selected composite sheets (1, 3 and 4)

3.2.2 General Full Factorial Design

The matrix design of the CR removal efficiency is demonstrated in **Table S2.** Plots of the main and interaction effects, the Pareto chart and the response optimizer were discussed laterally.

The main effects plots were displayed in **Fig 6** which determined the average deviation of each factor. Generally, the dye removal increased by increasing the deviation in the studied levels (Travlou et al 2013) and is considered as a negative effect on the removal percentage. Results reported in **Table S2** and **Fig 6** exhibited that the deviation increased from the low to the high levels. Furthermore, the CR concentration, sheet types (treats), contact time and dose have positive effects on the CR removal efficiency, which is indicated by the increase in the removal efficiency of these factors.

Generally, the interaction between the selected factors has positive and negative effects on pollutant removal efficiency (Ponnusami et al 2007). The data in **Table 1** and **Fig 7**, displayed that the interaction between the Congo red concentration & the sheet type (treats) has a significant effect on the removal efficiency. This attitude was also observed across the high result of P-value and through the non-parallel lines (Abdel-Ghani et al 2009).

Fig 8 exhibited the Pareto charts of the Congo Red (CR) removal efficiencies using the selected composite sheets (1, 3, and 4). The results were significant for all studied factors.

The obtained data agreed with the main and interaction effects, as reported previously (Mathialagan and Viraraghavan 2005).

In fact, the response optimizer normally predicts the optimum combined parameters that attain the highest pollutant removal efficiency (Bingol et al 2010). **Fig 9** demonstrated that applying 7 g/L doses of the composite sheet 1 for 240 min to 500 ppm CR, accomplished the highest CR removal efficiency of 76.27 % at a degree of accuracy 1.

3.3 Langmuir and Freundlich isotherms

Langmuir and Freundlich were used to investigate the CR adsorption mechanism (Abdelhamid et al 2023). Results displayed in **Figs 10 and 11** showed that the CR removal efficiency data was mostly fitted with the Freundlich isotherm for the composite sheets (1 and 3). In the case of the CR removal using the composite sheet 4, it was fitted well with the Langmuir isotherm. This result was appropriate to the higher R^2 that determines the fitted model as previously reported (Aksakal and Ucun 2010). Fitting the data to the Freundlich isotherm determines the mechanism of adsorption as heterogeneous adsorption with a multilayer adsorption nature

Table 2. Coefficient table of the selected composite sheets; 1, 3, 4 (treats) optimizations for the CR removal efficiency

Terms	Coef	SE Coef	T-Value	P-Value
Constant	73.804	0.124	595.81	0.000
CR Conc. (ppm)				
100	-1.023	0.124	-8.26	0.000
Composite sheets (Treat)				
1	-0.508	0.175	-2.90	0.012
3	0.490	0.175	2.80	0.015
Dose (g/l)				
2	-0.382	0.124	-3.08	0.009
Time				
30	-0.326	0.124	-2.63	0.021
CR Conc. (ppm)*Treat				
100 1	-0.771	0.175	-4.40	0.001
100 3	0.432	0.175	2.47	0.028
Composite sheets (Treat)*Time				
1 30	-0.321	0.175	-1.83	0.090
3 30	-0.005	0.175	-0.03	0.976
Dose (g/l)*Time				
2 30	0.252	0.124	2.04	0.063
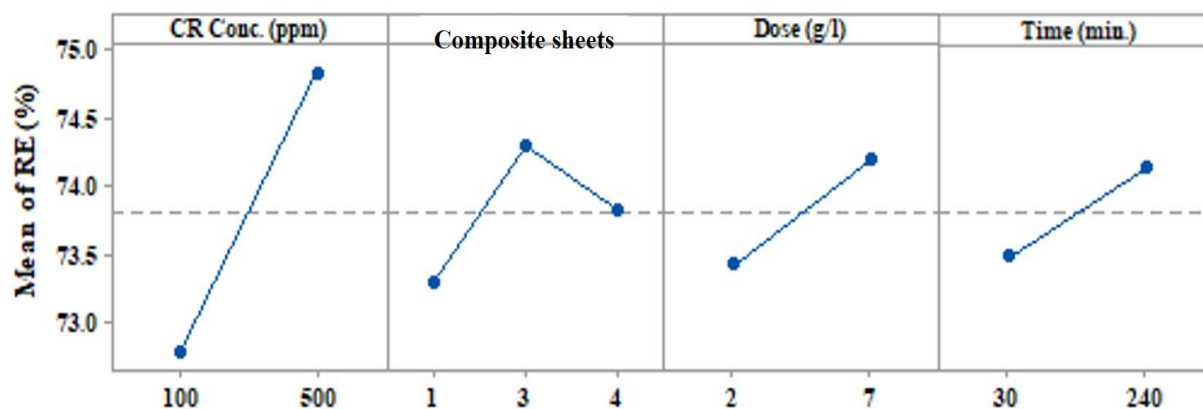
Fig 6. The main effect of the Congo red (CR) removal efficiencies using the selected composite sheets (1, 3 and 4)
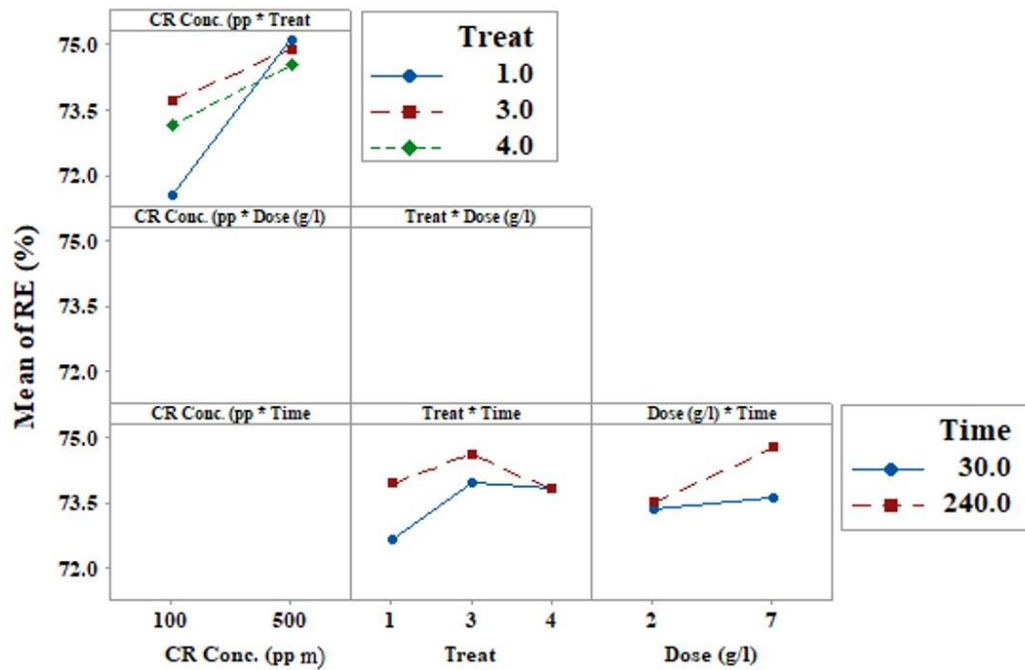
Fig 7. The interaction effect of the Congo Red (CR) removal efficiencies using the selected composite sheets (1, 3 and 4)
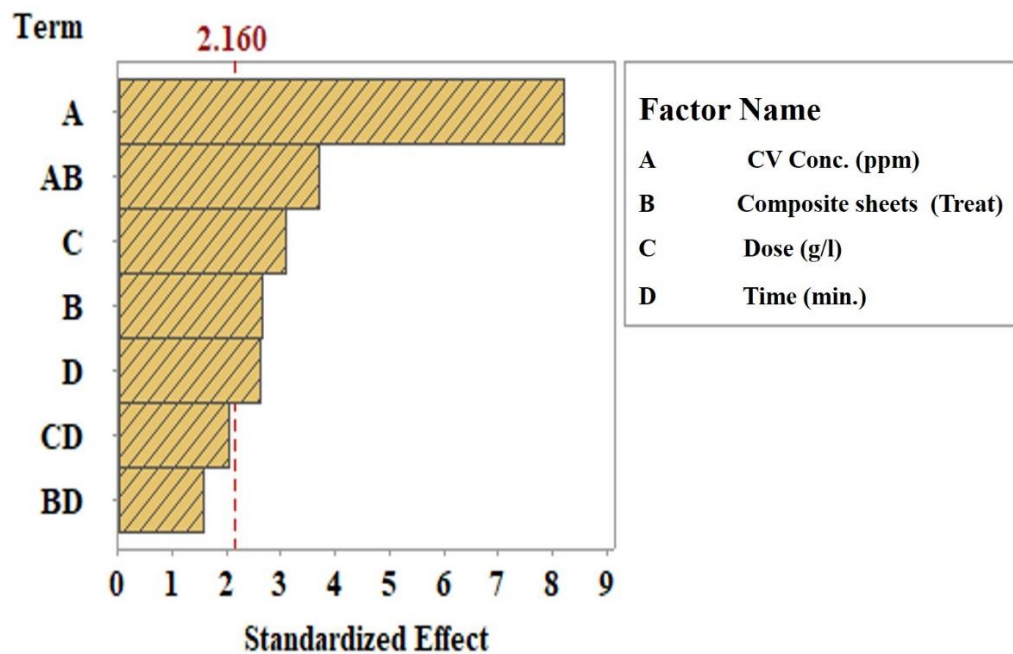

Fig 8. The Pareto charts of the Congo Red (CR) removal efficiencies using the selected composite sheets (1, 3, and 4)
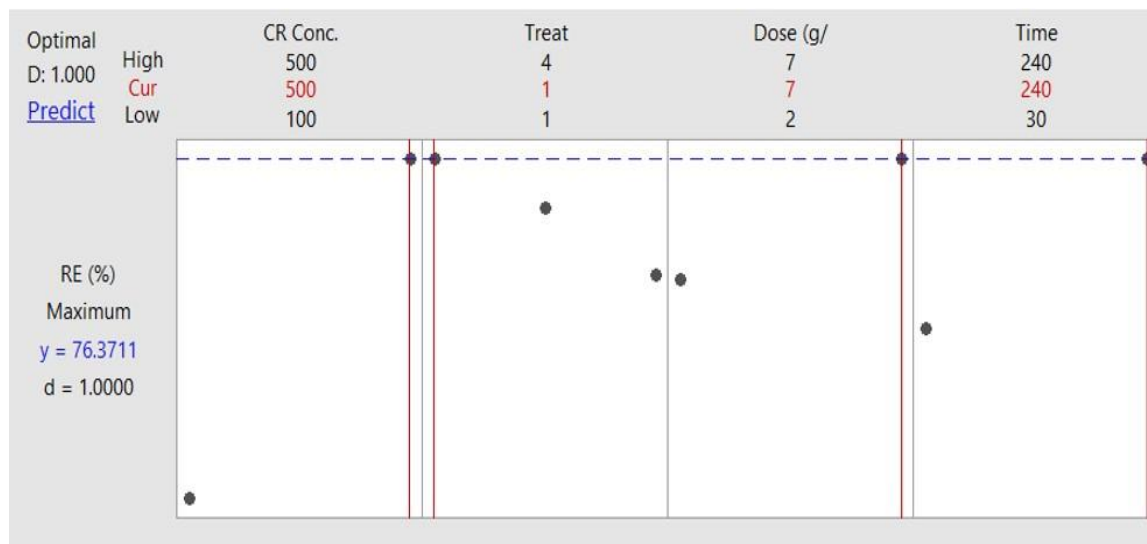
Fig 9. The Response optimizer of the Congo Red (CR) removal efficiencies using the selected composite sheets (1, 3, and 4)
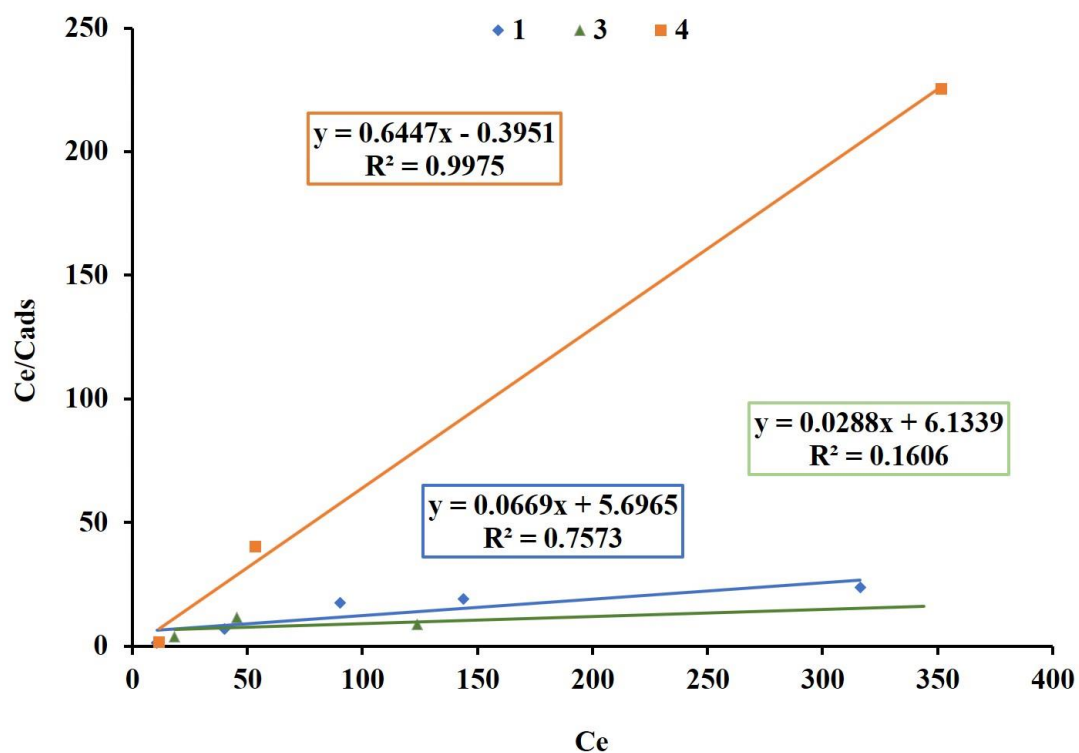

Fig 10. The Langmuir isotherm of the Congo Red (CR) removal efficiencies using the selected composite sheets (1, 3, and 4)
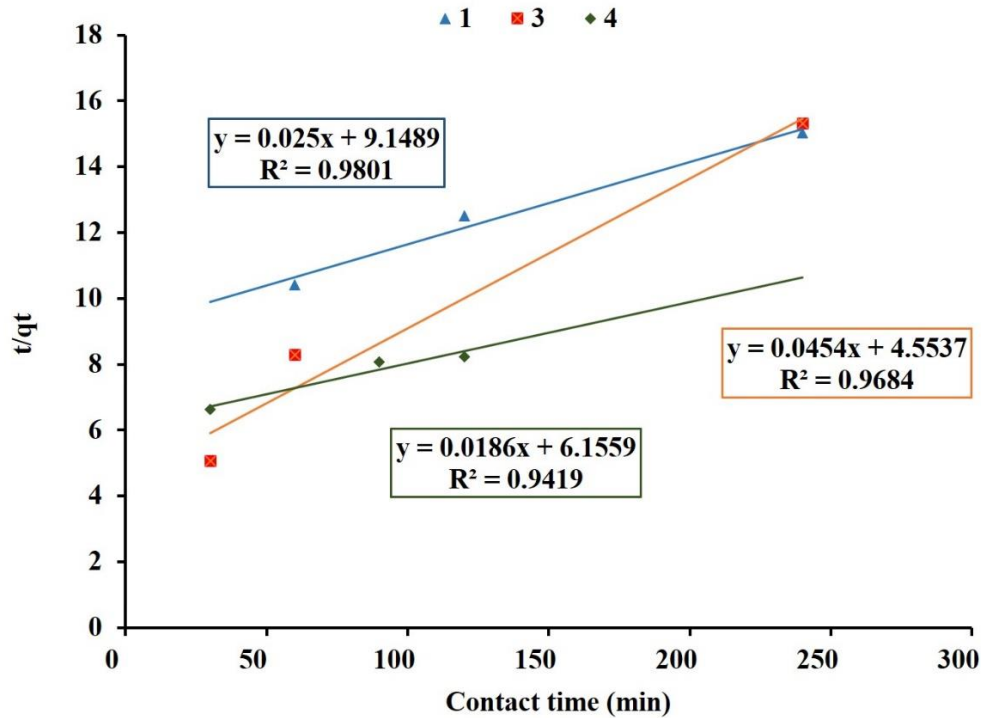
Fig 11. The Freundlich isotherm of the Congo Red (CR) removal efficiencies using the selected composite sheets (1, 3 and 4)

where wander Val's forces control the adsorption process. Nevertheless, Langmuir isotherm represents the adsorption mechanism as homogenous adsorption in nature i.e.; the pollutant adsorbed on the sorbent`s surface as far as no available sorbent`s active sites. The maximum adsorption capacity (Q_{max}) of the selected composite sheets (1, 3, and 4) was performed from unhydrolyzed bagasse wastes. were represented in **Table 3**.

Table 3. The Langmuir and Freundlich isotherms of the Congo Red (CR) removal efficiencies using the selected composite sheets (1, 3 and 4)

Langmuir isotherm			
	R^2	b	Q_{max}
1	0.76	0.0116	15.15
3	0.16	0.00326	50.00
4	0.99	1.53846	1.56
Freundlich isotherm			
	R^2	n	k
1	0.99	5.49451	11.48
3	0.80	0.8426	199.53
4	0.75	1.60668	97.72

3.4 Kinetic study

The Kinetics study is important to state the capacity of the selected composite sheets (1, 3, and 4) performed from unhydrolyzed bagasse wastes for removal of the CR. Results displayed in **Figs 12 and 13** and **Table 4** exhibited the kinetics plots in addition to their parameters. The correlation coefficient, R^2, indicated that the pseudo 2nd kinetic was the fitted model for the CR dye removal using the selected composite sheets (1, 3, and 4) performed from unhydrolyzed bagasse wastes. This result could be returned to the mentioned higher R^2 of the pseudo 2nd kinetic in addition to the result of the q_e calculated of the pseudo-order kinetics, which was near from the qe experimental, unlike the state of the pseudo-first-order (1st) reaction (Hang and He 2014).

3.5 Reusability experiment

Fig 14 demonstrates the reusability experiment. The highest efficient selected composite sheet (4) was applied successfully five times in the process of 3Rs (removal, recovery and reuse) (Abdelhamid et al 2023). Results obtained from the response optimizer were used to perform the reusability experiments. The results indicated that the removal efficiency of the CR was high in the first three runs and then declined in the fourth and fifth runs. The maximum removal efficiencies of 76.27% were achieved.
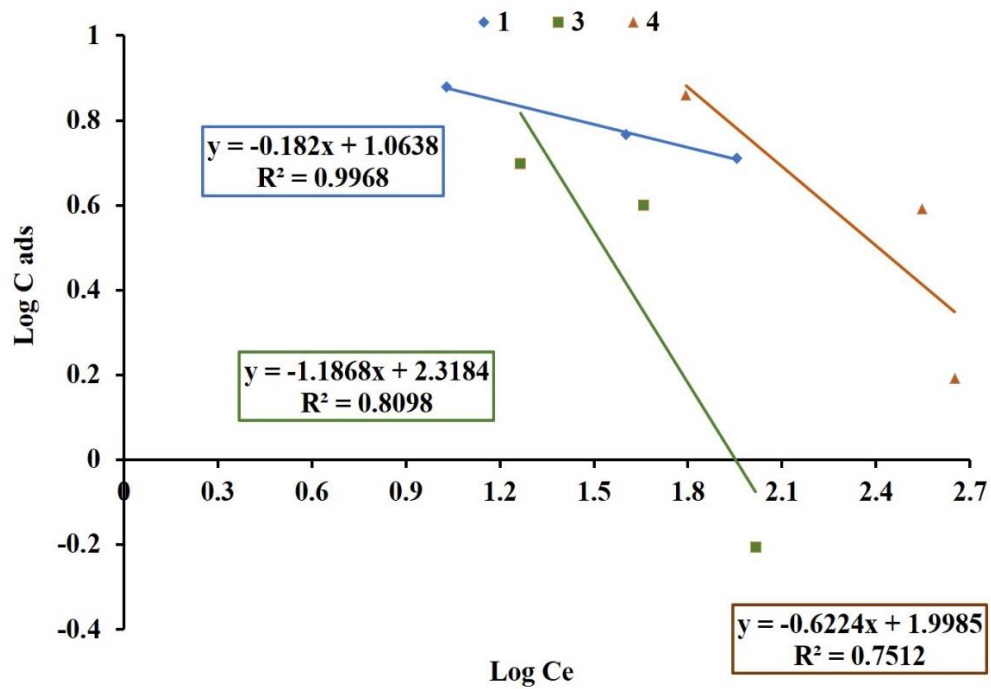
Fig 12. The first order (1st) kinetics study of the Congo Red (CR) removal efficiencies using the selected composite sheets (1, 3, and 4)
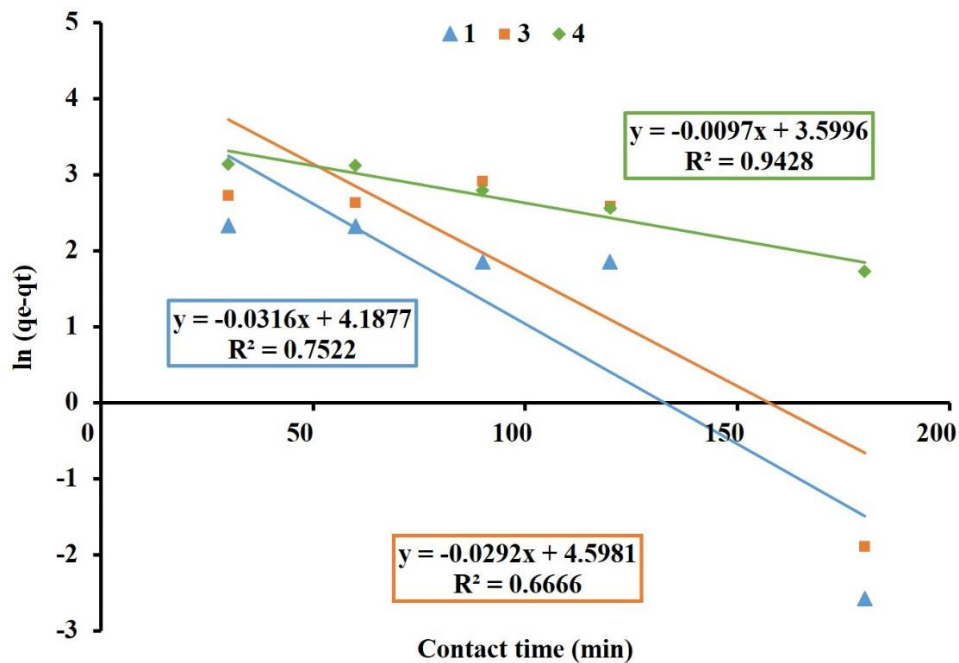

Fig 13. The second-order (2nd) kinetics study of Congo Red (CR) removal efficiencies using the selected composite sheets (1, 3, and 4)

Table 4. The first (1st) and the second (2nd) order kinetics of the Congo Red (CR) removal efficiencies using the selected composite sheets (1, 3 and 4)

1st order				
	R^2	**K**	**$Qe_{expr.}$**	**$Qe_{calc.}$**
1	0.39	0.00691	20.6	208.9
3	0.72	0.01474	32.34	2511.9
4	0.85	0.02027	37.9	3162.3
2nd order				
	R^2	**K**	**$Qe_{expr.}$**	**$Qe_{calc.}$**
1	0.9	0.000212	20.6	22.72727
3	0.89	0.000107	32.34	45.24887
4	0.85	9.99E-05	37.9	40.32258
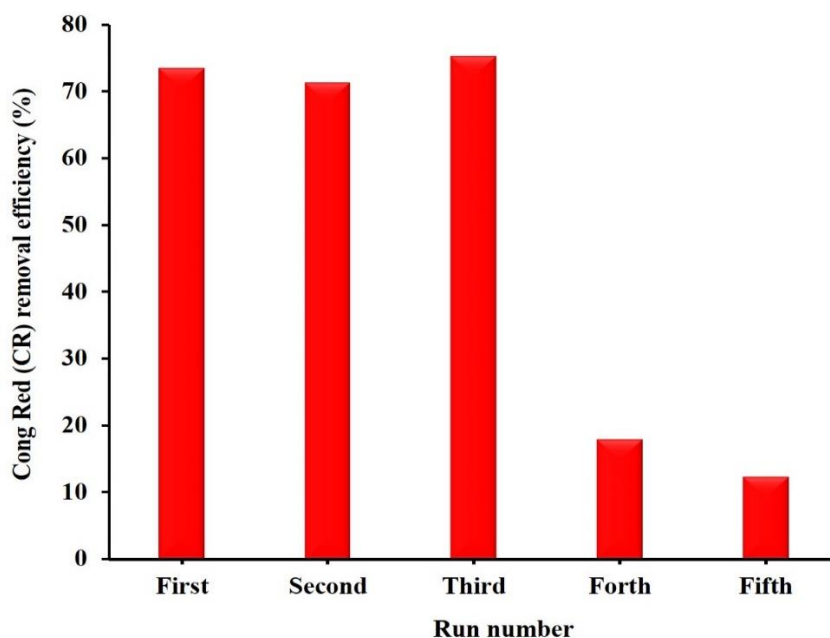
Fig 14. Reusability experiment of the highly efficient selected composite sheet performed from unhydrolyzed bagasse waste as 3Rs process (removal of Congo Red (CR), recovery it from the composite sheet and reuse the composite sheets for fifth times

4 Conclusion

The residual wastes, unhydrolyzed sugarcane bagasse wastes after acid treatment, were described as 1, 2, 3, 4 and control (only sugarcane bagasse waste without treatment. The unhydrolyzed sugarcane bagasse wastes were perfectly ground with ball milling, to increase their surface areas, and added to cellulose acetate to form five composite sheets. The composite sheets were used in the adsorption of Congo red from polluted water. The composite sheets of 1, 3 and 4 were selected from the screening test. The highest removal efficiencies of 76.27, 75.6 and 75.7 % for the composite sheet 1, 3 and 4, respectively for 500 ppm of the anionic dye Congo red (CO) were successfully achieved after 240 min of contact time, at a pH of 7.0 (the composite sheet`s concentration was of 7 g/L). Freundlich isotherm was fitted well

with the data obtained from CR removal efficacies using the selected composite sheets 1 and 3. In the case of CR removal using composite sheet 4, r.esults fitted well with the Langmuir isotherm. The correlation coefficient, R^2, indicated that the pseudo-second order (2nd) kinetics was the fitted model for the CR dye removal of the selected composite sheets (1, 3, and 4) performed from unhydrolyzed bagasse wastes. The highest efficient selected composite sheet was applied successfully five times in the process of 3Rs (Removal of CR using the composite sheet, Recover of the CR after removal using ethanol and reuse of the composite sheet many times) processes. For further investigation in the future, the composite sheets can be used through a reactor design for easy application of the removal process in the industrial and agriculture sectors.

References

Abdel-Ghani NT, Hegazy AK, El-Chaghaby GA, et al (2009) Factorial experimental design for biosorption of iron and zinc using *Typha domingensis* phytomass. *Desalination* 249, 343-347. https://doi.org/10.1016/j.desal.2009.02.065

Abdelhamid AE, Khalil AM (2019) Polymeric membranes based on cellulose acetate loaded with candle soot nanoparticles for water desalination. *Journal of Macromolecular Science, Part A* 56, 153–161. https://doi.org/10.1080/10601325.2018.1559698

Abdelhamid AE, Labena A, Mansor ES, et al (2023) Highly efficient adsorptive membrane for heavy metal removal based on *Ulva fasciata* biomass. *Biomass Conversion and Biorefinery* 13, 1691–1706. https://doi.org/10.1007/s13399-020-01250-7

Abo-State MA, Ragab AME, El-Gendy NSH, et al (2013) Effect of different pretreatments on Egyptian sugarcane bagasse saccharification and bioethanol production. *Egyptian Journal of Petroleum* 22, 161–167. https://doi.org/10.1016/j.ejpe.2012.09.007

Ajala EO, Ighalo JO, Ajala MA, et al (2021) Sugarcane bagasse: a biomass sufficiently applied for improving global energy, environment and economic sustainability. *Bioresources and Bioprocessing* 8, 87. https://doi.org/10.1186/s40643-021-00440-z

Aksakal O, Ucun H (2010) Equilibrium, kinetic and thermodynamic studies of the biosorption of textile dye (Reactive red 195) onto *Pinus sylvestris* L. *Journal of Hazardous Materials* 181, 666–672. https://doi.org/10.1016/j.jhazmat.2010.05.064

Alver E, Metin AÜ (2012) Anionic dye removal from aqueous solutions using modified zeolite: Adsorption kinetics and isotherm studies. *Chemical Engineering Journal* 200-202, 59–67. https://doi.org/10.1016/j.cej.2012.06.038

Beltrán-Heredia J, Sánchez-Martín J (2008) Azo dye removal by *Moringa oleifera* seed extract coagulation. *Coloration Technology* 124, 310–317. https://doi.org/10.1111/j.1478-4408.2008.00158.x

Bingol D, Tekin N, Alkan M (2010) Brilliant Yellow dye adsorption onto sepiolite using a full factorial design. *Applied Clay Science* 50, 315–321. https://doi.org/10.1016/j.clay.2010.08.015

Cho BP, Yang T, Blankenship LR, et al (2003) Synthesis and characterization of N-demethylated metabolites of malachite green and leucomalachite green. *Chemical Research in Toxicology* 16, 285–294. https://doi.org/10.1021/tx0256679

El-Jamal MM, Ncibi MC (2012) Biosorption of methylene blue by *Chaetophora elegans* algae: kinetics, equilibrium and thermodynamic studies. Acta Chimica Slovenica 59, 24–31. https://pubmed.ncbi.nlm.nih.gov/24061169/

Freundlich H (1907) Über die adsorption in lösungen. *Zeitschrift für Physikalische Chemie* 57, 385–470. https://doi.org/10.1515/zpch-1907-5723

Hang C, He J (2014) Study of the desorption of hydrolysed reactive dyes from cotton fabrics in an ethanol–water solvent system. *Coloration Technology* 130, 81–85. https://doi.org/10.1111/cote.12066

Ho YS, Ng JCY, Mckay G (2000) Kinetics of pollutant sorption by biosorbents: Review. *Separation and Purification Methods* 29, 189–232. https://doi.org/10.1081/SPM-100100009

Husien SH, Labena A, El Belely E, et al (2019a) Absorption of hexavalent chromium by green micro algae *Chlorella sorokiniana*: live planktonic cells. *Water Practice and Technology* 14, 515–529. https://doi.org/10.2166/wpt.2019.034

Husien SH, Labena A, El Belely E, et al (2019b) Adsorption studies of hexavalent chromium [Cr (VI)] on micro-scale biomass of *Sargassum dentifolium*, seaweed. *Journal of Environmental Chemical Engineering* 7, 103444. https://doi.org/10.1016/j.jece.2019.103444

Javadian H, Ahmadi M, Ghiasvand M, et al (2013) Removal of Cr (VI) by modified brown algae *Sargassum bevanom* from aqueous solution and industrial wastewater. *Journal of the Taiwan Institute of Chemical Engineers* 44, 977–989. https://doi.org/10.1016/j.jtice.2013.03.008

Kamran U, Bhatti HN, Noreen S, et al (2022) Chemically modified sugarcane bagasse-based biocomposites for efficient removal of acid red 1 dye: Kinetics, isotherms, thermodynamics and desorption studies. *Chemosphere* 291, 132796. https://doi.org/10.1016/j.chemosphere.2021.132796

Kant R (2012) Textile dyeing industry an environmental hazard. *Natural Science* 4, 22–26. https://doi.org/10.4236/ns.2012.41004

Langmuir I (1918) The adsorption of gases on plane surfaces of glass, mica and platinum. *Journal of the American Chemical Society* 40, 1361–1403. https://doi.org/10.1021/ja02242a004

Mathialagan T, Viraraghavan T (2005) Biosorption of pentachlorophenol by fungal biomass from aqueous solutions: A factorial design analysis. *Environmental Technology* 26, 571–580. https://doi.org/10.1080/09593332608618542

Moghazy RM (2019) Activated biomass of the green microalga *Chlamydomonas variabilis* as an efficient biosorbent to remove methylene blue dye from aqueous solutions. *Water SA* 45, 20–28. http://dx.doi.org/10.4314/wsa.v45i1.03

Moghazy RM, Labena A, Husien SH (2019) Eco-friendly complementary biosorption process of methylene blue using micro-sized dried biosorbents of two macro-algal species (*Ulva fasciata* and *Sargassum dentifolium*): Full factorial design, equilibrium, and kinetic studies. *International Journal of Biological Macroleculesn* 134, 330–343. http://dx.doi.org/10.1016/j.ijbiomac.2019.04.207

Morán-Aguilar MA, Calderón-Santoyo M, de Souza Oliveira RP, et al (2022) Deconstructing sugarcane bagasse lignocellulose by acid-based deep eutectic solvents to enhance enzymatic digestibility. *Carbohydrate Polymers* 298, 120097. https://doi.org/10.1016/j.carbpol.2022.120097

Munagapati VS, Wen JC, Pan CL (2020) Adsorptive removal of anionic dye (Reactive Black 5) from aqueous solution using chemically modified banana peel powder: kinetic, isotherm, thermodynamic, and reusability studies. *International Journal of Phytoremediation* 22, 267–278. https://doi.org/10.1080/15226514.2019.1658709

Nandi BK, Goswami A, Purkait MK (2009) Removal of cationic dyes from aqueous solutions by kaolin: Kinetic and equilibrium studies. *Applied Clay Science* 42, 583–590. https://doi.org/10.1016/j.clay.2008.03.015

Ponnusami V, Krithika V, Madhuram R, et al (2007) Biosorption of reactive dye using acid-treated rice husk: factorial design analysis. *Journal of Hazardous Materials* 142, 397-403. https://doi.org/10.1016/j.jhazmat.2006.08.040

Prabhu M, Davamani V, Gopitha G, et al (2017) Biosorption of chromium from tannery effluent using bacterial and fungal species. *Madras Agricultural Journal* 104, 148–151. http://dx.doi.org/10.29321/MAJ.04.000420

Rafatullah M, Sulaiman O, Hashim R, et al (2010) Adsorption of methylene blue on low-cost adsorbents, a review. *Journal of Hazardous Materials* 177, 70–80. https://doi.org/10.1016/j.jhazmat.2009.12.047

Travlou NA, Kyzas GZ, Lazaridis NK, et al (2013) Graphite oxide/chitosan composite for reactive dye removal. *Chemical Engineering Journal* 217, 256–265. https://doi.org/10.1016/j.cej.2012.12.008

Weber WJ, Morris JC (1963) Kinetics of adsorption on carbon from solution. *Journal of the Sanitary Engineering Division* 89, 31–59. https://doi.org/10.1061/JSEDAI.0000430